International Research Journal of Engineering and Technology (IRJET) e-ISSN: 2395-0056
Volume: 10 Issue: 06 | Jun 2023 www.irjet.net p-ISSN: 2395-0072

Evolution of the Physico-Mechanical Properties of Calcined Clay Cement from Different Sources of Kaolin Clay

Aya R. Abdelfattah[1], Abdelrahman Ragab[2], Shaimaa Younis[3], Magdy Elymany[4]

[1]MSc. Student, Civil Engineering Department, Faculty of Engineering, Fayoum University, Fayoum 63514, Egypt
[2]Lecturer of Chemistry, Department of Basic Science, Future Institute for Engineering, Fayoum, Egypt
[3]Lecturer, Civil Engineering Department, Future Institute for Engineering, Fayoum, Egypt
[4]Professor, Civil Engineering Department, Faculty of Engineering, Fayoum University, Fayoum 63514, Egypt

---

Abstract - *The development of binders based on limestone and calcined clays appears to be a promising way to increase the substitution of clinker. Their production is likely to remain limited if highly kaolinitic clays are required, but calcined clays with low metakaolin content are less reactive in a binder, as shown in many previous studies. This study focused on the differences, regarding hydration degree and products, between several binders containing two types of calcined clay and limestone filler. Two calcined clays were studied, coming from two very different raw clays. The first calcined clay contained more metakaolin than the second one. In this article, we produced the LC3 from two clays. The production of LC3 used 10, 15, 22.5, and 30% of calcined clay, 10 % of limestone filler, and 5% gypsum. This was also studied by using one type of each calcined clay individually. Binary binders showed strong differences between the two calcined clays. However, this work showed significant pozzolanic activity and synergy between calcined clay and limestone filler in the binder. This observation was made even for the composite calcined clay with minor metakaolinite content. From this comprehensive study on hydration, it can be concluded that calcined clay with low metakaolin content is likely to result in the same degree of hydration and products over the long term as high metakaolin calcined clay in a binary system, The LC3 formed from CC Zafarana and CC of Sinai was better than OPC, especially in the durability. cement pastes were investigated by the determination of water of consistency (W/C, %), setting times (STs), and compressive strength (CS). Some selected cement pastes were identified using XRD, TG and DTA techniques to show the hydration products with curing time.*

Key Words: Limestone calcined clay cement (LC3), CC=MK, Clinker partial replacement, Environmental Impact, Compressive strength, Microstructure.

1.INTRODUCTION

In recent years, the world's attitude in all fields has changed to go green. Due to the recent high records of the carbon footprint, many industries have turned to green manufacturing or processing. One of the most affecting industries on air pollution is cement production. This industry participates with large scale in the CO_2 emissions as recorded around 6% of the global warming causes [1–5]. The cement production waste not only emits many harmful substances that can harm the human's respiratory system, such as slag, ashes, cement dust, marble dust, etc…., but also, they have a very high disposal cost [6]. Moreover, no matter how important cement is in our world, this production consumes an extreme amount of energy [7]. As a result, the cement industry stakeholders initiated new approaches to eliminate the waste from the beginning like replacing the cement with some sustainable alternatives with green impact on the environment; however, these replacement alternatives showed undesired results of the mechanical strengths of the cement [4]. Another opinion states that the cement industry wastes themselves can be recycled and result in higher superior mechanical properties and structure life, in this work [2], cement kiln dust and fly ash are reused to optimize the Portland cement. Many researches address the full or partial replacement of cement because of the previously mentioned reasons [8–17]. Therefore, Researchers introduced new ternary cementitious system called limestone calcined clay cement (LC3) that is a combination of ordinary Portland cement (OPC), limestone and calcined clay extracted from various regions around the world such as China [18,19], Brazil [17,20], North America, South Asia [21], Cuba [22] and Argentina [23]. This attracted the researchers' interest to study the physico-mechanical properties of the new (LC3) concrete mixtures in order to present a sufficient final product that competes with the OPC mixtures. It is found that when the clay is calcined, metakaolin is formed that in turn react with calcium hydroxide producing C-A-S-H and aluminate hydrates. Then, the reaction between the alumina and the limestone produces carbo-aluminate hydrates. Eventually, all these reactions fill the porous spaces in the structure that lead to the improvement of the physico-mechanical properties of the cement [24–26].

Huang et al. [18] studied the development of LC3 paste that includes a calcined clay from Maoming, China. The study showed that early strengths of LC3 (before 7 days) tends to be lower than the OPC concrete, however, late strengths show remarkable strength increase compared to OPC, especially the flexural and splitting tensile strengths, due to the secondary reaction of the amorphas silica and alumina.

In addition, the LC3 bond-slip behavior with steel bars is identical to the OPC behavior and failure modes. The fast reaction of calcined clay resulted a well refined and less porous microstructure of the LC3 mixture, though, this affected the strength of the material as there was no strength increase after 28 days [27]. In addition, a study provided that 30% to 45% of LC3 content achieves comparable mechanical properties to the OPC cement from curing age of 7 days onwards, especially in the 30% LC3 mixture [28].

Nair et al. [29] uncovered that the partial replacement of the cement with the limestone calcined clay (LC2) system achieves desired workability as long as the LC2 percentage remains less than 30%. Also, long travel times are unlikely wanted on the construction site which is confirmed by Sánchez et al. [22] that more than 100km travel between clay deposit and site is undesirable. Furthermore, a study on LC2 using D-optimal mixture design (DMD) showed that the limestone and calcined clay content can reach 56.8% of the cementitious system mixture, although achieving desirable flowability and mechanical properties compared to OPC paste [30]. Moreover, five calcined clays from different areas were investigated and examined. This study concluded that the compressive strength of the LC3 system can outperform the OPC cement by 40% increase because of the involvement of calcine clay (up to 40%) in the refinement of the porosity of the structure [21]. Despite increasing the limestone and calcined clay contents in the cementitious mixture, the expansion rate of the mortar decreases alongside with the dynamic modulus loss under sulfate attack up to 270 days due to the reactive alumina in the calcined clay that react with the limestone to produce less porous structure [31].

Higher dosage of blended LC3 cement (50-80%) contributed to lower compressive strengths, particularly >60%, however, 50% participation of LC3 attained sufficient compressive strength compared to OPC 52.5N as per BS EN197-1, in addition to better environmental impact and lower cost [32].

In this research, the partial replacement of cement approach is followed. In order to reduce the cement content in the concrete, two novel calcined clays from Egypt are blended with the OPC paste to produce a new LC3 paste. The two LC3 pastes with different weight contents (wt% of OPC) alongside with the OPC paste are experimented and tested. The preparation of the cement mixtures is illustrated in detail. The mechanical tests include compressive strength, flexural strength and splitting tensile strength. Also, the X-ray diffraction analysis (XRD) is carried out in addition to the differential scanning calorimetry analysis (DSC) and Thermal Gravimetric Analysis (TGA).

2. EXPERIMENTAL WORK

In this section, the materials used in this research are presented. In addition, the equipment used for the material preparation and testing are provided.

2.1 Materials

A limestone calcined clay cement (LC3) consisting of limestone, calcined clay, see Figure 1, and Portland cement clinker was used. Cement contains limestone of 10%, calcined clay up to 30%, and the remaining are Portland clinker with fixed 5% of gypsum. The used limestone is a high-grade from quarry of Lafarge Cement Company as shown in Figure 1a. Properties of the raw materials are given in **Table 1.** Limestone and Zaafarana was prepared in an industrial kiln of clinker in Lafarge Cement Company. High-efficient grinding was carried out to obtain MK. The Blaine surface area of Metakaolin was 4500 cm2/g. The XRD phases of K and MK are given in Table 1. Also, see Figure 2, the XRD patterns K and MK show that the MKS more reactive than MKZ. The chemical oxide composition of Portland cement and MK is given in Table 2, and the Mineralogical composition of OPC is given in Table 3.

Figure 1: LC3 components; (a) high-grade limestone and (b) calcined clay (metakaolin).

Table 1: The XRD phases of K and MK.

Sample Name	R_{wp}	Alite Sum	Lime	Periclase	Quartz	Anhydrite	Calcite	Mullite	Magnetite	Hematite	Thernadite	Rutile	Silica amorph
KZ	8.94	2.17	0.05	0.18	42.34	2.2	2.51	3.18	0.38	2.9	1.75	1.12	41.21
MKZ	19.12	1.64	0.88	1.18	0.4	0	0	5.21	0	0	0.54	14.6	75.54
KS	61.39	0.1	1.48	0	14.87	2.7	0.59	0.74	3.11	0.37	0	0.27	75.76
MKS	5.09	0	0.14	0.17	11.37	1.45	0.32	0.51	0	0.2	0	0.14	85.68

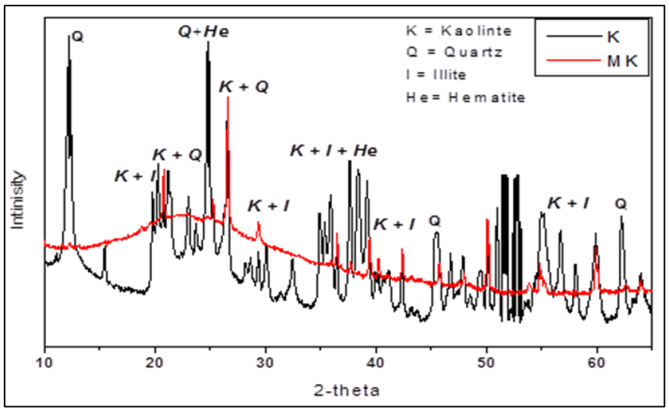

Figure 2: XRD pattern of K and MK

Table 2: The oxide composition and properties of raw materials.

Ingredient	Percentage (%)				
	OPC	KZ	MKZ	KS	MKS
Silica (SiO_2)	20.58	62.59	68.04	45.67	53.59
Alumina (Al_2O_3)	4.46	16.74	20.59	34.34	39.75
Iron Oxide (Fe_2O_3)	4.02	6.24	8.01	0.33	0.38
Lime (CaO)	64.02	1.59	2.02	0.34	0.42
Magnesia (MgO)	3.57	0.73	0.82	0.04	0.04
Sulfur trioxide (SO_3)	1.59	0.40	0.42	0.00	0
Potassium oxide (K_2O)	0.34	0.52	0.68	0.05	0.07
Sodium oxide (Na_2O)	0.51	0.36	0.49	0.01	0.01
Chlorine (Cl)	0.1	0.15	0.01	0.0	0.0
Loss of ignition (LOI)	3.1	8.42	0.45	12.95	0.35

Table 3: The mineralogical composition of OPC.

Ingredient	Percentage (%)
Tricalcium silicate (C_3S)	58.38
Dicalcium silicate (C_2S)	14.98
Tricalcium aluminate (C_3A)	5.03
Tetracalcium aluminoferrite (C_3AF)	12.22

In this study, the composition of the cement mixture is illustrated in Table 4. Generally, the mix design of the cement is the OPC cement with added fine aggregates and coarse in addition to the water content wt. (%) to cement.

Table 4: Mix Design of Concrete.

Cement (kg/m^3)	Fine Aggregates (kg/m^3)	Coarse (kg/m^3)	Water (w/c)
320	790	1080	0.55

The aim of this research is to partially replace OPC cement with limestone calcined clay (LC3). In this work, two calcined clays extracted from two different desert regions in Egypt; Zaafarana and Sinai, are investigated. The experimented mixtures are normal OPC, Zaafarana LC3 of 7.5, 15, 22.5 and 30 wt.% of cement and Sinai LC3 of 7.5, 15, 22.5 and 30 wt.% of cement as shown in Table 5. Hence, the experiment includes 9 mixtures given the names OPC, $LC3_{S1}$ to $LC3_{S4}$ for Sinai LC3 and $LC3_{Z1}$ to $LC3_{Z4}$ for Zaafarana LC3.

Table 5: Blending Composition of Cement

Mix		Clinker (%)	Gypsum (%)	Calcined Clay (%)	Limestone (%)
OPC		95	5	0	0
$LC3_{S1}$	$LC3_{Z1}$	77.5	5	7.5	10
$LC3_{S2}$	$LC3_{Z2}$	70	5	15	10
$LC3_{S3}$	$LC3_{Z3}$	62.5	5	22.5	10
$LC3_{S4}$	$LC3_{Z4}$	55	5	30	10

The experiment is carried out on two different types of calcined clays, in addition to the OPC cement. The samples for each mixture are 15 cubes of 15 x 15 x 15 cm (3 for each curing age), 2 standard cubes 10 x 10 x 10 cm, 4 cylinders of diameter 15 cm and 30 cm height (2 for 28 days and 2 for 90 days), and 4 beams of square cross-section of 10 cm and 50 cm length (2 for 28 days and 2 for 90 days), see Figure 3. The nine mixtures are tested after five curing ages 2,7, 28, 56 and 90 days for cube samples and two curing ages 28 and 90 for cylinder samples and beam samples. The tests carried out in this research are mechanical testing, Differential Scanning Calorimetry (DSC) and Thermal Gravimetric Analysis (TGA), Scanning Electron Microscope (SEM) and X-Ray Diffraction (XRD).

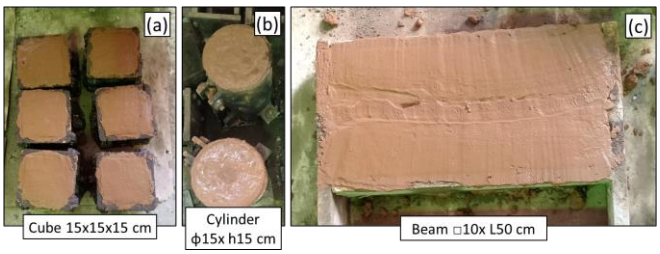

Figure 3: Prepared mixture sample (a) cubes, (b) cylinders and (c) beams.

2.2 Mechanical Testing

The compressive strengths are obtained by ADR Touch SOLO 2000 compression machine (ELE International, England) as shown in Figure 4. The ADR machine implies the compressive strengths as follows,
The cube samples compressive strength is calculated by Eq. (1),

$$\sigma_c = \frac{P_{failure}}{A} \quad (1)$$

Where $P_{failure}$ is the peak (failure) compressive force, and A is the cube contact surface area.
Also, the in-direct tensile stress of the cylinder samples is calculated by Eq. (2).

$$f_t = \frac{2P_{failure}}{\pi DH} \quad (2)$$

Where D is the cylinder diameter and H is the cylinder height.
Finally, the flexural strength of beam samples is obtained by Eq. (3).

$$f_b = \frac{P_{failure}L}{bd^2} \quad (3)$$

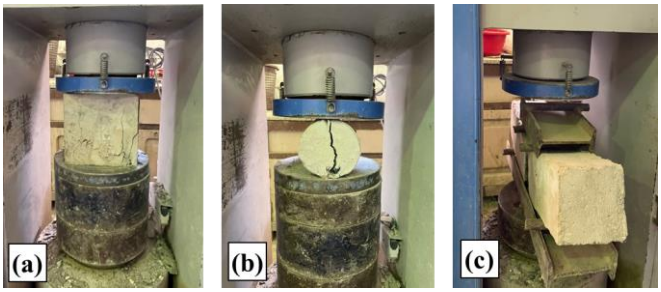

Figure 4: The mechanical testing on ADR machine (a) compressive strength, (b) in-direct tensile stress and (c) flexural strength.

2.3 Differential Scanning Calorimetry (DSC) and Thermal Gravimetric Analysis (TGA)

The DSC and TGA tests are carried out by Simultaneous Thermal Analyzer (STA) 6000 in N_2 atmosphere (Perkin-Elmer, USA). The DSC test identifies some useful properties such as temperature of phase changes in the material. Meanwhile, the TGA test measures the change in weight (%) versus the temperature or time and determines various phases in the concrete. Both tests are performed at a rate of 10 °C/min up to 1000 °C on samples of 10 mg.

2.4 X-Ray Diffraction (XRD)

The powder method of XRD of some selected hardened cement pastes was adopted in the present study to identify the different crystalline phases. The x-ray diffraction evaluation is conducted on Empyrean (Malvern Panalytical, Malvern, United Kingdom). The X-ray tube voltage and current were fixed at 40.0 KV and 30.0 mA respectively. The measurement conditions are shown in Table 6.

Table 6: XRD measurement conditions.

Item	Description
Device Model	Empyrean
Step Size [°2θ]	0.0130
Scan Step Time [s]	3.57
Temperature [°C]	25
Anode Material	Cu
K-Alpha1 [Å]	1.54060
K-Alpha2 [Å]	1.54443
K-Beta [Å]	1.39225
K-A2 / K-A1	0.5
Generation Specs.	30 mA, 40 kV

3. RESULTS AND DISCUSSION

3.1 Water Consistency and Setting times

The results of the water consistency and setting times of the investigated cement pastes with different LC3 are shown in Figure 5 and Table 7. The results show that the water consistency of LC3 increases slightly with increased calcined clay (CC) content up to 30 wt. %, which is mainly attributed to the increase of surface area and decrease of crystal lattice in cement clinker phases. The initial and final setting times are slightly elongated by an increase in CC of up to 30 wt. %. This is due to two factors: the first is the increase in mixing water, and the second is the dilution of the cement clinker by the CC portion and low percentage of $Ca(OH)_2$ [17,18].

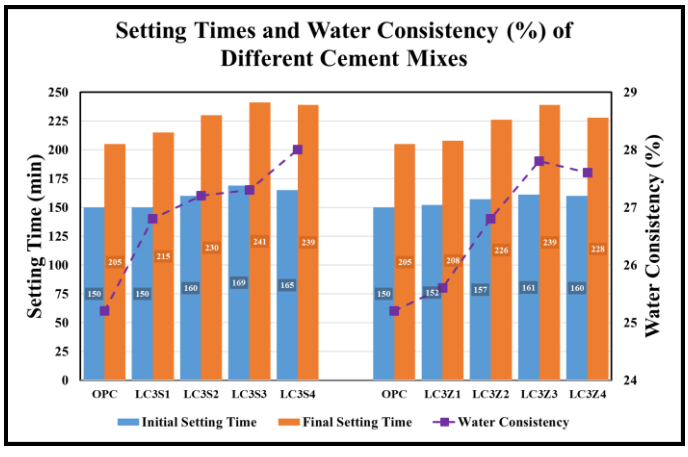

Figure 5: Setting times and water consistency of different cement mixtures.

Table 7: Water consistency and setting times of design mixtures.

Mix	Water Consistency (%)	Setting Times (mins)	
		Initial	Final
OPC	25.2	150	205
$LC3_{S1}$	26.8	150	215
$LC3_{S2}$	27.2	160	230
$LC3_{S3}$	27.3	169	241
$LC3_{S4}$	28	165	239
$LC3_{Z1}$	25.6	152	208
$LC3_{Z2}$	26.8	157	226
$LC3_{Z3}$	27.8	161	239
$LC3_{Z4}$	27.6	160	228

3.2 Mechanical Properties

3.2.1 Compressive Strength

The compressive strengths of cube samples (15x15x15 cm) at all curing ages for all mixtures are obtained in **Table 8** and Figure 6. The results are calculated as the average of the 3 cube samples at each curing age. These results show a promising partial replica of OPC, as the compressive strength of $LC3_{Z4}$ is higher than that of OPC by 2%. It is observed that the compressive strength increases proportionally with the increase in the LC3 formed from the Sinai CC percentage in all curing ages. On the other hand, the compressive strength of LC3 of Zaafarana CC tends to decrease at 7.5%, then increase until 30% at all curing ages. The fluctuations in compressive strengths for both Sinai and Zaafarana LC3 mixtures at all curing ages are presented in Figure 7. The results show that the compressive strength of $LC3_{Z4}$ at 90 days is the best at 52 MPa. Also, increasing the calcined clay percentage from 7.5% to 30% (ignoring the base value of OPC) is proportional to the compressive strength [35], [36].

Table 8: Average compressive strength in (MPa) of hardened concrete samples.

Mix	2 Days	7 Days	28 Days	56 Days	90 Days
OPC	21.3	30.4	47.1	48.9	51
$LC3_{S1}$	26	35.8	45.6	47.6	50
$LC3_{S2}$	27.3	35.9	45.5	47.5	50.1
$LC3_{S3}$	26.2	37.4	45.9	47.9	50.6
$LC3_{S4}$	25.1	38.8	45.7	48	50.9
$LC3_{Z1}$	13.4	27.2	42.9	44.1	45.5
$LC3_{Z2}$	13.6	27.7	44.2	47	50.5
$LC3_{Z3}$	14.1	27.5	43.9	47.2	51.3
$LC3_{Z4}$	14.6	27.3	43.5	47.4	52

The results show that at an early curing age, the compressive strength of LC3 formed from CC of Z is higher than that of LC3 formed from CC of S, which is opposite at a later curing age. These results are due to the CC of Sinai containing a higher percentage of alumino silicate amorphous phase than the CC of Zafferana, but with longer curing times due to more hydration products, heat of hydration, and other minerals, they produce Portland $Ca(OH)_2$, which is reacted with the reaming of the aluminosilicate phase by a complexed reaction to give CSH. Also, nucleation sites to reactivity and improve packing as well as their pozzolanic reactivity [37]. Therefore, the LC3 formed from CC Zafferana is better than CC Sinai in terms of durability.

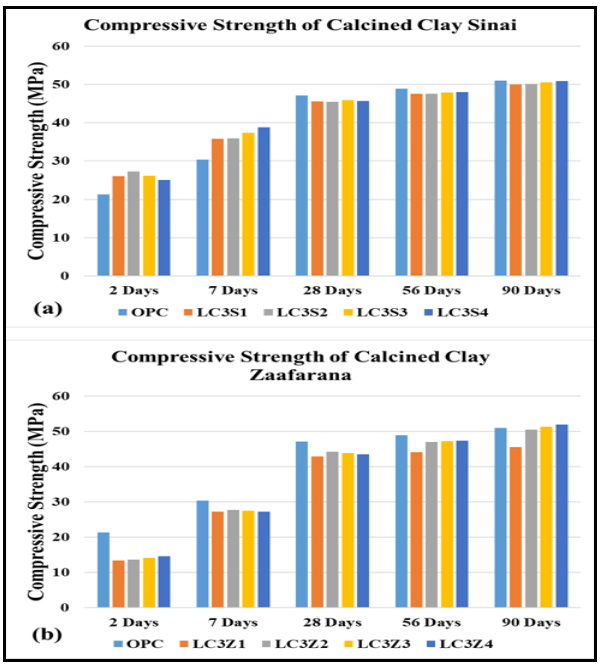

Figure 6: Compressive strengths at different curing ages for (a) Sinai LC3 and (b) Zaafarana LC3.

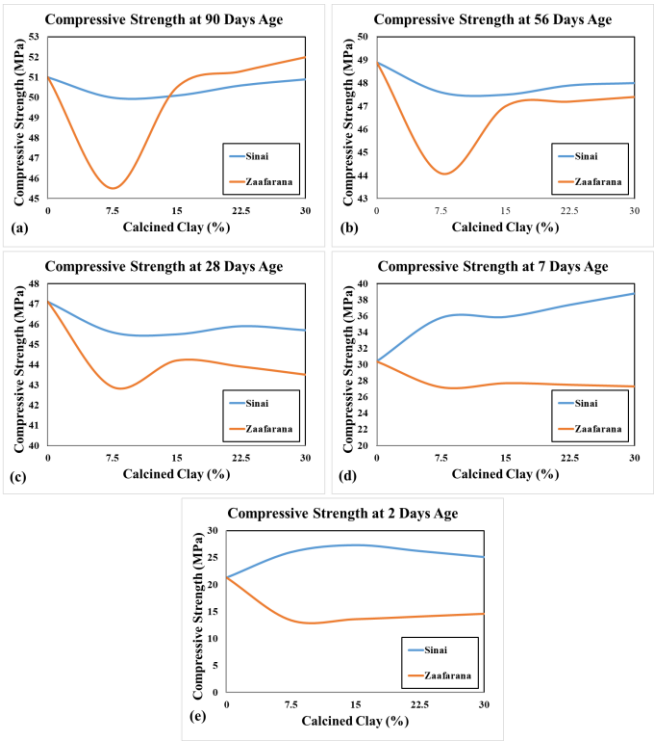

Figure 7: Compressive strength comparison between Sinai and Zaafarana LC3 at (a) 90 days, (b) 56 days, (c) 28 days, (d) 7 days, (e) 2 days.

3.2.2 In-Direct Tensile Strength (Splitting Strength)

The indirect tensile strengths of cylinder samples (ϕ15 and height 30 cm) are obtained at curing ages of 28 and 90 days, as shown in **Table 9**. In order to visualise the proportion between the CC percentage and the indirect tensile strength of both Sinai and Zaafarana clays, the strengths are plotted in **Figure 8**. Apparently, the $LC3_{Z1}$ mixture weakens the strength of the cement, as presented previously in Figure 7. However, the recorded results entail that the best indirect tensile strength is 6.6 MPa at $LC3_{Z3}$ at 90 days, followed by $LC3_{Z4}$ at 90 days by 6.59 MPa and $LC3_{S3}$ at 90 days by 6.54 MPa. In this work, the splitting strength is 12.74% of the compressive strength of the material. Therefore, the LC3 formed from CC Zaafarana and CC of Sinai was better than OPC in durability.

Table 9: Indirect tensile strength (MPa) of cylinder samples.

Mix	28 days	90 days
OPC	6.03	6.50
$LC3_{S1}$	5.75	6.40
$LC3_{S2}$	5.75	6.43
$LC3_{S3}$	5.94	6.54
$LC3_{S4}$	5.86	6.56
$LC3_{Z1}$	5.45	6.30
$LC3_{Z2}$	5.59	6.39
$LC3_{Z3}$	5.65	6.60
$LC3_{Z4}$	5.45	6.59

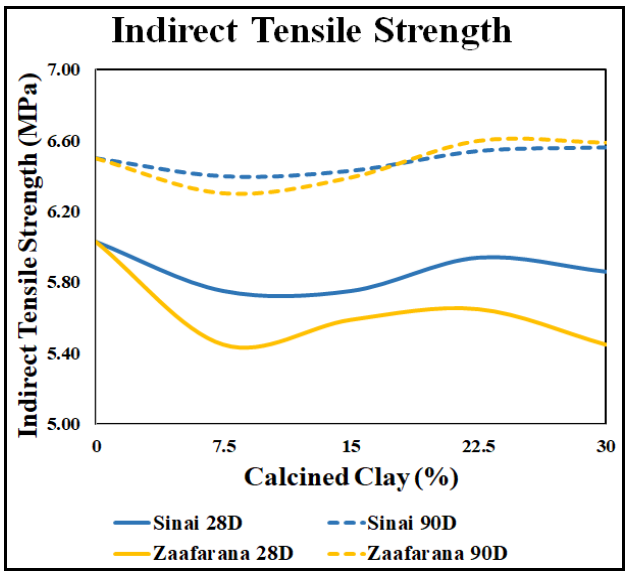

Figure 8: The indirect tensile strength of different mixtures at 28 and 90 days of both Sinai and Zaafarana calcined clays.

3.2.3 Flexural Strength

Table 10 shows the results of the flexural strength test at curing ages of 28 and 90 days for both Sinai and Zaafarana LC3 beam samples of the same dimensions (square cross-section of 10 cm and a length of 50 cm). The best recorded flexural strength after the base mixture (OPC) is $LC3_{Z4}$ at the age of 90 days, at 8.94 MPa (1.7% better than OPC). Inevitably, the $LC3_{Z1}$ mixture affects the strength of the material negatively, as shown in **Figure 9**. It is observed that the flexural strength of the material is around 17% of the compressive strength. However, the differences in the flexural strengths between OPC and the samples of $LC3_{Z4}$ and $LC3_{S4}$ are negligible, as they are within 1.4% of the maximum of the OPC flexural strength.

Table 10: Flexural strength (MPa) of beam samples

Mix	28 days	90 days
OPC	8.12	8.79
$LC3_{S1}$	7.88	8.64
$LC3_{S2}$	7.64	8.61
$LC3_{S3}$	7.76	8.76
$LC3_{S4}$	7.80	8.89
$LC3_{Z1}$	7.33	7.77
$LC3_{Z2}$	7.47	8.63
$LC3_{Z3}$	7.49	8.76
$LC3_{Z4}$	7.31	8.94

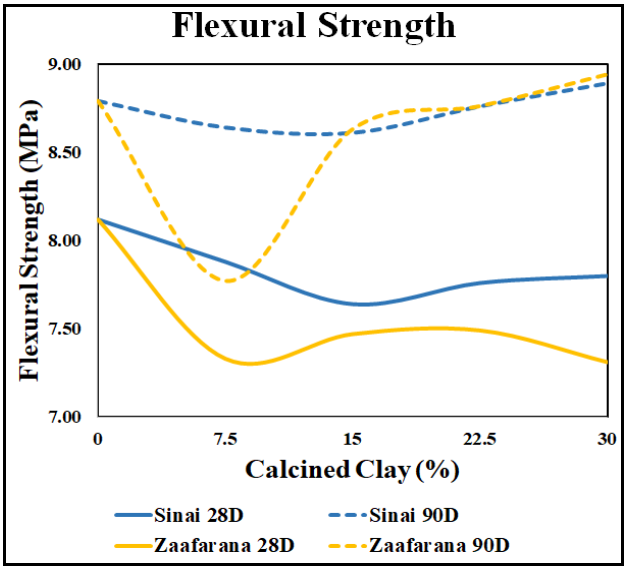

Figure 9: Flexural strength of different mixtures at 28 and 90 days of both Sinai and Zaafarana calcined clays.

To wrap up, the results of the mechanical tests show promising alternatives to Portland cement (OPC), regardless of the slight differences in the mechanical properties. Fruitfully, the production of clinker will be reduced by 22.5% to 30%, which, in turn, will reduce air pollution from the carbon emissions of cement industries and increase the sustainability and durability of concrete. The reaction of alumino-silicate elements in CC with CH and hydroxide in cement leads to the addition of bond strength and solid volume. Increase of the content of CC leads to an increase in strength, this is due to the continuous hydration as well as the formation of additional C–S–H (the main source of compressive strength) and C–A–S–H hydrates.

3.3 XRD Analysis

From the X-ray diffractograms, it is clearly evident that the limestone and calcined systems lead to the formation of carboaluminate phases. These phases tend to be present at an early age (28 days), as shown in the diffractogram, and are stable in the system even at 28 days. In that respect, the carboaluminate phase becomes one of the major phases in the cement hydrate system. Additionally, the density of these phases is on the lower side within the cement hydrate system. Furthermore, stabilization of ettringite (again in a low-density phase) occurs with the formation of the carboaluminates, as shown in the semi-quantitative evaluation. These additional phases could alter the microstructure, which is clearly evident from the pore structure results. Early refinement of pore structure suggests that the LC3 cementitious system has a highly refined microstructure and the existence of a new phase assemblage, which still needs a better understanding.

Figure 10 illustrates the XRD-patterns of hydrated OPC paste after curing for 28 and 90 days. The patterns show the remaining parts of clinker minerals, namely β-C_2S and C_3S, up to 28 and 90 days of hydration, respectively. It is obvious that the relative intensities of their peaks decrease with curing time, up to 90 days more than 28 days, as a result of their hydration. Also, the peaks of the portlandite (CH) phase increase with curing time due to the hydration of the silicate phases of OPC clinker with the formation of C-S-H and the liberation of CH. The CSH is overlapped by the peaks of $CaCO_3$. The calcite can be formed by the reaction of atmospheric CO_2 with the CH [38].

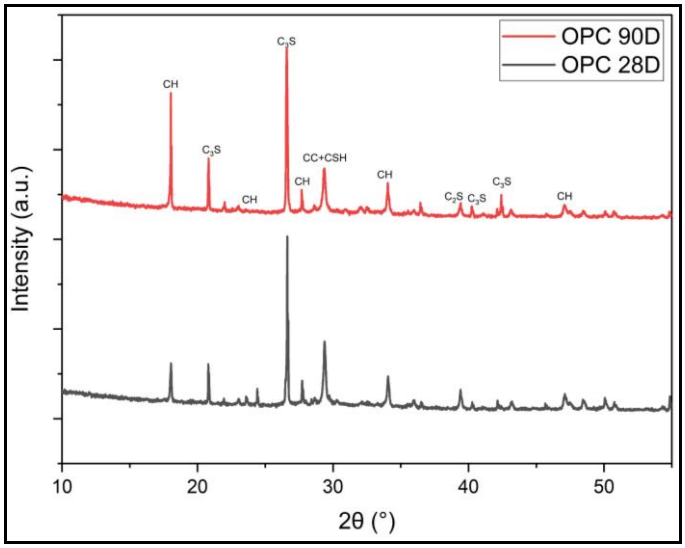

Figure 10: The XRD-patterns of hydrated OPC paste after curing ages 28 and 90 days.

Figure 11 illustrates the XRD-patterns of hydrated $LC3_{S2}$, $LC3_{Z2}$ and OPC paste after curing ages of 28 and 90 days. The patterns show the remaining parts of clinker minerals, namely β-C_2S and C_3S, up to 28 and 90 days of hydration, respectively. It is obvious that the relative intensities of their peaks decrease with curing time up to 28 days as a result of their hydration. Also, the peaks of the portlandite (CH) phase increase with curing time due to the hydration of the silicate phases of OPC clinker with the formation of C-S-H and the liberation of CH. The CSH is overlapped by the peaks of $CaCO_3$. The calcite can be formed by the reaction of atmospheric CO_2 with the CH. It is clear that in OPC but in LC3 at 28 days, the peaks of the portlandite (CH) phase are disappearing in $LC3_{S2}$ due to the pozzolanic reaction of CC Sinai with (CH). The peaks of the portlandite (CH) phase are also lower in $LC3_{Z2}$ than in OPC. At 90 days, all portlandite (CH) phases are consumed in both types of LC3 due to pozzolanic reactions [39].

Figure 12 illustrates the XRD-patterns of hydrated $LC3_{S4}$, $LC3_{Z4}$ and OPC paste after curing ages of 28 and 90 days, respectively. The patterns illustrate that anhydrous phases of clinker minerals C_2S and C_3S still exist up to 28 and 90 days; their peak intensities decrease with curing time. Also, the intensities of the peaks of portlandite decrease with curing time due to the pozzolanic reaction of CC with the liberation of Portlandite. The patterns show that the intensities of portlandite peaks of LC3 from Zaafarana clay paste are higher than those of LC3-Portland from Sinai clay cement pastes due to the pozzolanic reaction of CC with CH.

The intensity of calcite ($CaCO_3$) peaks decreases with CC contents; this is an indication of the consumption of CH by CC, which is the source of carbonation. It is also obvious that the increase in CC content leads to more consumption of CH [40].

Figures (13-14) illustrates the XRD patterns of hydrated LC3 from Sinai clay and hydrated LC3 from Zaafarana clay, respectively, at curing ages 28 and 90 days. The patterns show that the intensities of portlandite peaks in LC3 from Zaafarana clay paste are higher than those of LC3 from Sinai clay paste due to the pozzolanic reaction of CC with CH. The intensity of calcite (CaCO3) peaks decreases with CC contents; this is an indication of the consumption of CH by CC, which is the source of carbonation. It is also obvious that the increase in CC content leads to more consumption of CH [41]. The results of this test show that LC3 of Sinai clay is more reactive than LC3 of Zaafarana clay, especially at early ages.

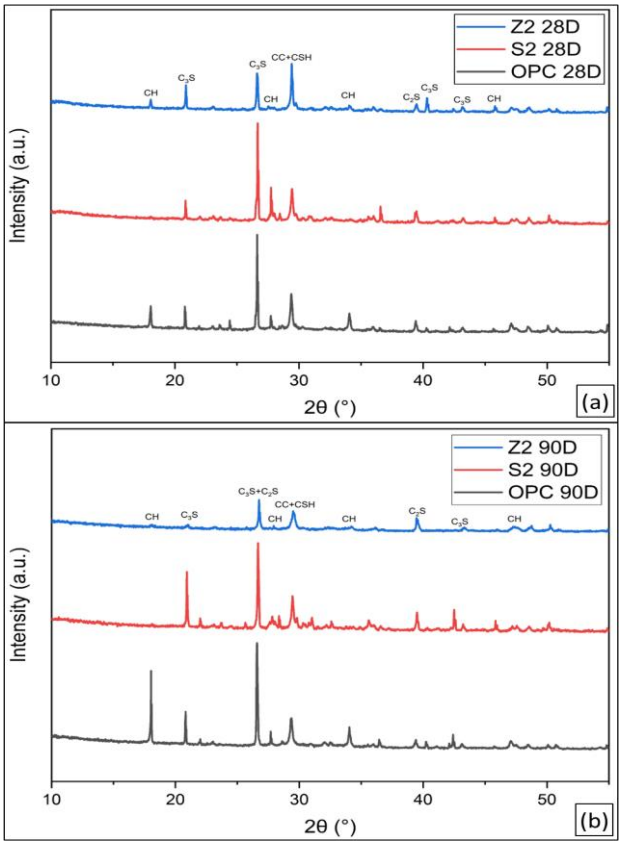

Figure 11: The XRD-patterns of hydrated $LC3_{S2}$ and $LC3_{Z2}$ paste after curing ages (a) 28 days, (b) 90 days.

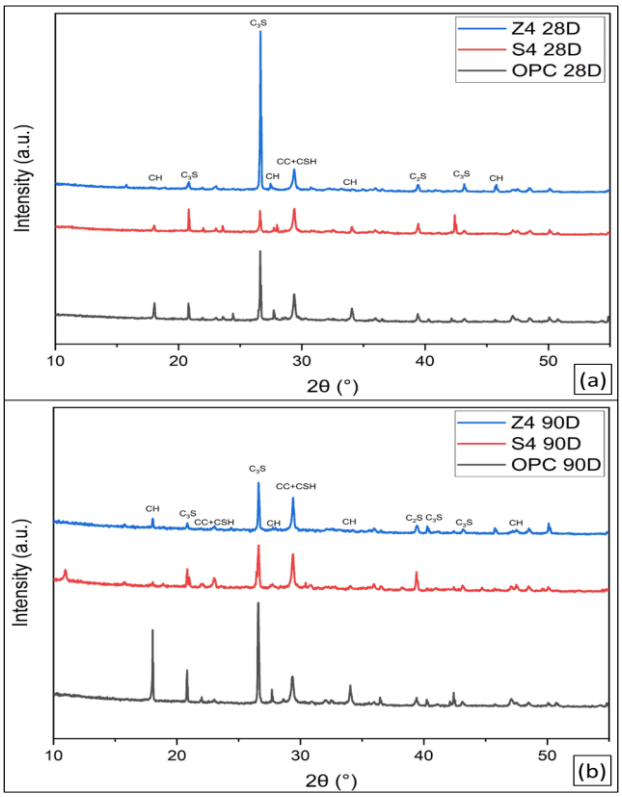

Figure 12: The XRD-patterns of hydrated $LC3_{S4}$ and $LC3_{Z4}$ paste after curing ages (a) 28 days, (b) 90 days.

3.4 DSC and TGA Analysis

Figure 15 illustrates the DSC/TGA thermograms of the hydrated OPC and both Sinai and Zaafarana LC3 pastes cured for up to 90 days. The DTA thermograms show the occurrence of three endothermic peaks at 120, 420–450, and 700–750 °C for both clays in Figs. 15a and 15b. The endothermic peak located below 200 °C is mainly due to the dehydration of interlayer water of CSH, whereas the endothermic peak at 420–450 °C is due to the dehydroxylation of $Ca(OH)_2$. The last endothermic peak located at 700–750 °C is due to the decomposition of $CaCO_3$. It is clear that the intensities of the endothermic peaks characteristic for $Ca(OH)_2$ increase with curing time up to 90 days in OPC due to the progress of hydration of OPC pastes. Also, the endothermic peaks of CSH increase with curing time due to the progress of hydration. The hydration progress can be studied using thermogravimetric analysis (TGA). The weight loss of the hydrated phases without $Ca(OH)_2$ and $CaCO_3$ increases with curing time.

The TG losses characteristic for the hydration products at low temperatures (up to 200 °C) are at 90 days, more than 28 days, and more than 2 days. This means that the degree of hydration increases with curing time. On the other hand, the TG losses characteristic for portlandite (CH) are at 90 days, which is less than 28 days and less than 2 days. The increase in TG loss of portlandite with curing time is due to the continuous liberation of CH as a result of hydration of OPC. The TG losses due to the decomposition of $CaCO_3$ are at 90 days, less than 28 days, and less than 2 days. Also, the TG losses due to CaCO3 decrease with curing time; due to the reaction of CO_2 and moisture with $CaCO_3$ forming $Ca(HCO_3)_2$.

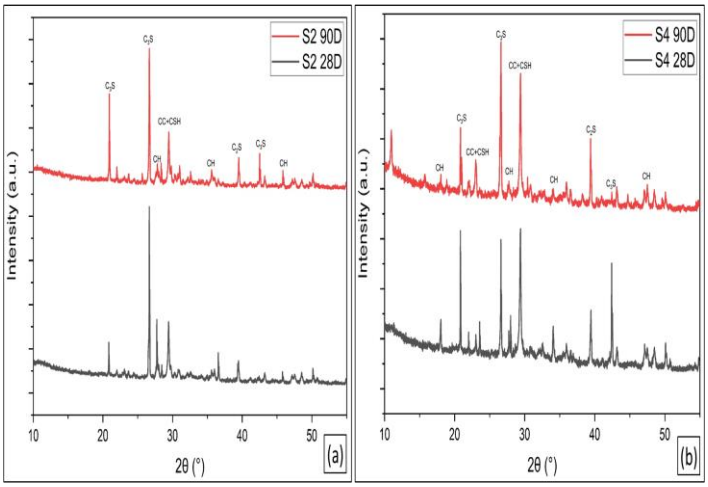

Figure 13: The XRD-patterns of hydrated (a) $LC3_{S2}$ paste, (b) $LC3_{S4}$ paste.

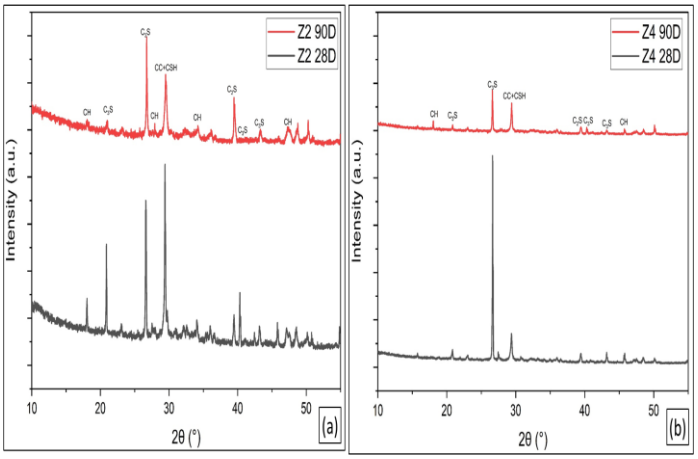

Figure 14: The XRD-patterns of hydrated (a) LC3Z2 paste, (b) LC3Z4 paste.

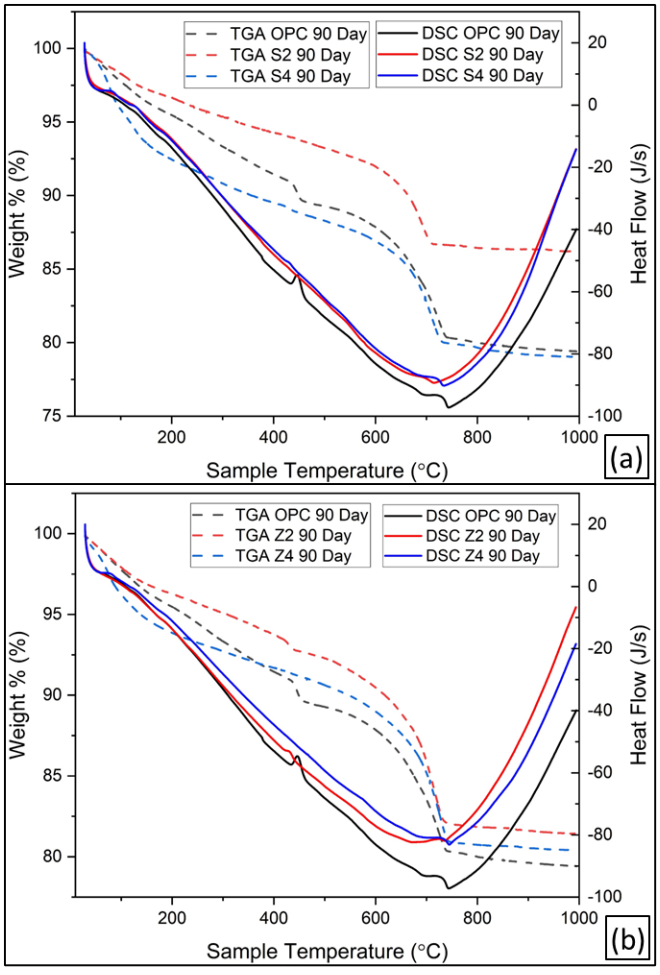

Figure 15: The DSC/TGA thermograms of the hydrated OPC cured for 90 days and compared to (a) Sinai LC3 paste, (b) Zaafarana LC3 paste.

The DTA/DTG thermograms of hydrated LC3 for both Sinai and Zaafarana clays of pozzolanic cement paste at curing age

up to 28 days are shown in Figure 16. Evidently, there are four endothermic peaks. The first weak endothermic peak located below 100 °C is mainly due to the removal of free water and the decomposition of the amorphous part of CSH gel. The second endothermic peak observed at about 120–140 °C represents the dehydration of the crystalline part of C-S-H, CAH, and CASH as well as the presence of gehlenite hydrates. The third endotherm, located at about 450 °C is due to the dehydroxylation of calcium hydroxide (CH). The last endothermic peak located at 700–710 °C is due to the decomposition of $CaCO_3$. It is clear that the second endothermic peak, located at about 130 °C increases with curing time due to the formation of excessive amounts of CAH and CASH as well as crystalline CSH. These phases are formed as a result of the hydration of OPC phases as well as the pozzolanic reaction of CC with CH.

The losses were decreased with LC3 content due to the formation of a low C/S ratio of C-S-H, which has a lower water content. Generally, the combined water content of OPC is lower than that of pozzolanic LC3 cement paste. The weight losses of LC3 cement paste at about 450 °C are 90 days, less than 28 days, and less than 2 days; these are due to the decomposition of portlandite CH. The decrease in weight loss with time is mainly due to the pozzolanic reaction of CC with CH [42].

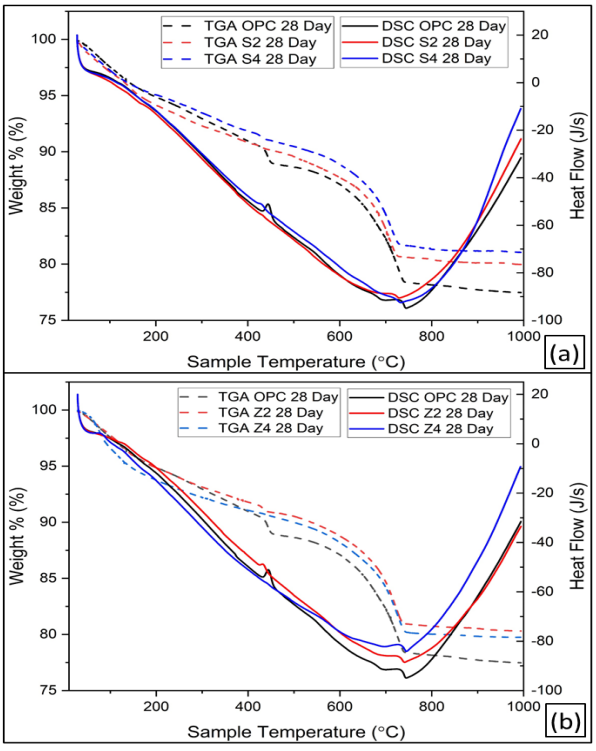

Figure 16: The DSC/TGA thermograms of the hydrated OPC cured for 28 days and compared to (a) Sinai LC3 paste, (b) Zaafarana LC3 paste.

4. CONCLUSIONS AND FUTURE WORK

The studied binary and ternary binders are based on Portland cement, calcined clays, and limestone filler. Low metakaolinitic calcined clay obtained from illite-kaolinite composite raw clay is compared with high kaolinite raw clay, which is mainly composed of metakaolin after calcination. The study aims at investigating the influence of composite calcined clay on the hydration of cement in binary. Advanced experimental techniques were combined to identify and quantify the hydration products at different ages. The findings are as follows;

1. The compressive strengths of Zaafarana calcined clay mixtures show promising mechanical behavior compared to the OPC cement as $LC3_{Z4}$ recorded best compressive strength of 52 MPa and flexural strength of 8.94 MPa at curing age of 90 days, meanwhile the $LC3_{Z3}$ entails the best indirect tensile strength of 6.60 MPa at curing age of 90days.

2. In the short term, the first calcined clay containing mainly CC (Sinai) showed a higher reactivity than the second composite calcined clay obtained from illite and kaolinite (Zaafarana). Even though the first calcined clay reacted faster in a cementitious matrix, it was demonstrated that the composite calcined clay did not slow down the hydration reactions of the clinker.

3. The composite calcined clay combined with limestone had a very positive impact on hydration. The pozzolanic reaction was actually improved when compared with the highly metakaolinite clay. The composite clay (illite/kaolinite) finally ages, and it has a higher pozzolanic activity than the highest metakaolin content. This shows that pure kaolinite raw clay is not necessarily required as the synergy between limestone filler and illite-kaolinite calcined clay can clearly be observed. The hydration of clinker phases and the phase assemblage of the cementitious matrix are influenced by the substitution of cement by calcined clay and limestone filler.

4. The reactivity of belite is lowered, but other phases are generated, such as aluminum-modified calcium silicate hydrate (C-A-S-H), strätlingite, and carboalumination in the presence of limestone and composite calcined clay. These phases can be expected to enhance the engineering properties of the materials for a given cement content.

5. At longer term, it was shown that behaviors tend to be similar even though pozzolanic activity was slightly higher for CC than composite calcined clay. The two types of calcined clay tended to have similar pozzolanic activity, especially in later ages.

ACKNOWLEDGEMENT

The authors can acknowledge Lafarge Egypt cement company for providing the raw materials of this research. Also, the authors acknowledge Fayoum University Materials laboratory for their help in conducting the mechanical testing.

REFERENCES

[1] E. Batuecas, I. Ramón-Álvarez, S. Sánchez-Delgado, and M. Torres-Carrasco, "Carbon footprint and water use of alkali-activated and hybrid cement mortars," *Journal of Cleaner Production*, vol. 319, p. 128653, Oct. 2021, doi: 10.1016/j.jclepro.2021.128653.

[2] S. M. Bagheri, M. Koushkbaghi, E. Mohseni, S. Koushkbaghi, and B. Tahmouresi, "Evaluation of environment and economy viable recycling cement kiln dust for use in green concrete," *Journal of Building Engineering*, vol. 32, p. 101809, Nov. 2020, doi: 10.1016/j.jobe.2020.101809.

[3] A. Ababneh, F. Matalkah, and R. Aqel, "Synthesis of kaolin-based alkali-activated cement: carbon footprint, cost and energy assessment," *Journal of Materials Research and Technology*, vol. 9, no. 4, pp. 8367–8378, Jul. 2020, doi: 10.1016/j.jmrt.2020.05.116.

[4] Y. Zhao, J. Qiu, J. Xing, and X. Sun, "Chemical activation of binary slag cement with low carbon footprint," *Journal of Cleaner Production*, vol. 267, p. 121455, Sep. 2020, doi: 10.1016/j.jclepro.2020.121455.

[5] J. Yu, D. K. Mishra, C. Hu, C. K. Y. Leung, and S. P. Shah, "Mechanical, environmental and economic performance of sustainable Grade 45 concrete with ultrahigh-volume Limestone-Calcined Clay (LCC)," *Resources, Conservation and Recycling*, vol. 175, p. 105846, Dec. 2021, doi: 10.1016/j.resconrec.2021.105846.

[6] A. B. M. A. Kaish, T. C. Odimegwu, I. Zakaria, and M. M. Abood, "Effects of different industrial waste materials as partial replacement of fine aggregate on strength and microstructure properties of concrete," *Journal of Building Engineering*, vol. 35, p. 102092, Mar. 2021, doi: 10.1016/j.jobe.2020.102092.

[7] D. Suarez-Riera, L. Restuccia, and G. A. Ferro, "The use of Biochar to reduce the carbon footprint of cement-based materials," *Procedia Structural Integrity*, vol. 26, pp. 199–210, 2020, doi: 10.1016/j.prostr.2020.06.023.

[8] D. Taoukil, Y. El meski, M. lhassane Lahlaouti, R. Djedjig, and A. El bouardi, "Effect of the use of diatomite as partial replacement of sand on thermal and mechanical properties of mortars," *Journal of Building Engineering*, vol. 42, p. 103038, Oct. 2021, doi: 10.1016/j.jobe.2021.103038.

[9] Y. Kocak, "Effects of metakaolin on the hydration development of Portland–composite cement," *Journal of Building Engineering*, vol. 31, p. 101419, Sep. 2020, doi: 10.1016/j.jobe.2020.101419.

[10] R. Homayoonmehr, A. A. Ramezanianpour, and M. Mirdarsoltany, "Influence of metakaolin on fresh properties, mechanical properties and corrosion resistance of concrete and its sustainability issues: A review," *Journal of Building Engineering*, vol. 44, p. 103011, Dec. 2021, doi: 10.1016/j.jobe.2021.103011.

[11] N. Makul and P. Sokrai, "Influences of fine waste foundry sand from the automobile engine-part casting process and water-cementitious ratio on the properties of concrete: A new approach to use of a partial cement replacement material," *Journal of Building Engineering*, vol. 20, pp. 544–558, Nov. 2018, doi: 10.1016/j.jobe.2018.09.004.

[12] Y. Han, R. Lin, and X.-Y. Wang, "Performance and sustainability of quaternary composite paste comprising limestone, calcined Hwangtoh clay, and granulated blast furnace slag," *Journal of Building Engineering*, vol. 43, p. 102655, Nov. 2021, doi: 10.1016/j.jobe.2021.102655.

[13] I. Rodríguez Pérez, G. Vasconcelos, P. B. Lourenço, P. Quintana, C. García, and A. Dionísio, "Physical-mechanical characterization of limestones from Yucatan churches, Mexico," *Journal of Building Engineering*, vol. 44, p. 102895, Dec. 2021, doi: 10.1016/j.jobe.2021.102895.

[14] H. Berkak, M. Bederina, and Z. Makhloufi, "Physico-mechanical and microstructural properties of an eco-friendly limestone mortar modified with styrene-polyacrylic latex," *Journal of Building Engineering*, vol. 32, p. 101463, Nov. 2020, doi: 10.1016/j.jobe.2020.101463.

[15] Z. Zhao, A. Grellier, M. El Karim Bouarroudj, F. Michel, D. Bulteel, and L. Courard, "Substitution of limestone filler by waste brick powder in self-compacting mortars: Properties and durability," *Journal of Building Engineering*, vol. 43, p. 102898, Nov. 2021, doi: 10.1016/j.jobe.2021.102898.

[16] A. R. Lopes dos Santos, M. do R. da Silva Veiga, A. M. dos Santos Silva, and J. M. Caliço Lopes de Brito, "Tensile

bond strength of lime-based mortars: The role of the microstructure on their performance assessed by a new non-standard test method," *Journal of Building Engineering*, vol. 29, p. 101136, May 2020, doi: 10.1016/j.jobe.2019.101136.

[17] T. C. Cardoso, P. R. de Matos, L. Py, M. Longhi, O. Cascudo, and A. P. Kirchheim, "Ternary cements produced with non-calcined clay, limestone, and Portland clinker," *Journal of Building Engineering*, vol. 45, p. 103437, Jan. 2022, doi: 10.1016/j.jobe.2021.103437.

[18] Z. Huang *et al.*, "Development of limestone calcined clay cement concrete in South China and its bond behavior with steel reinforcement," *J. Zhejiang Univ. Sci. A*, vol. 21, no. 11, pp. 892–907, Nov. 2020, doi: 10.1631/jzus.A2000163.

[19] T. R. Muzenda, P. Hou, S. Kawashima, T. Sui, and X. Cheng, "The role of limestone and calcined clay on the rheological properties of LC3," *Cement and Concrete Composites*, vol. 107, p. 103516, Mar. 2020, doi: 10.1016/j.cemconcomp.2020.103516.

[20] C. Salvi Malacarne, M. Rubens Cardoso da Silva, S. Danieli, V. Gonçalves Maciel, and A. Paula Kirchheim, "Environmental and technical assessment to support sustainable strategies for limestone calcined clay cement production in Brazil," *Construction and Building Materials*, vol. 310, p. 125261, Dec. 2021, doi: 10.1016/j.conbuildmat.2021.125261.

[21] H. Maraghechi, F. Avet, H. Wong, H. Kamyab, and K. Scrivener, "Performance of Limestone Calcined Clay Cement (LC3) with various kaolinite contents with respect to chloride transport," *Mater Struct*, vol. 51, no. 5, p. 125, Oct. 2018, doi: 10.1617/s11527-018-1255-3.

[22] S. Sánchez Berriel *et al.*, "Assessing the environmental and economic potential of Limestone Calcined Clay Cement in Cuba," *Journal of Cleaner Production*, vol. 124, pp. 361–369, Jun. 2016, doi: 10.1016/j.jclepro.2016.02.125.

[23] A. Rossetti, T. Ikumi, I. Segura, and E. F. Irassar, "Sulfate performance of blended cements (limestone and illite calcined clay) exposed to aggressive environment after casting," *Cement and Concrete Research*, vol. 147, p. 106495, Sep. 2021, doi: 10.1016/j.cemconres.2021.106495.

[24] K. Scrivener, F. Martirena, S. Bishnoi, and S. Maity, "Calcined clay limestone cements (LC3)," *Cement and Concrete Research*, vol. 114, pp. 49–56, Dec. 2018, doi: 10.1016/j.cemconres.2017.08.017.

[25] C. Rodriguez and J. I. Tobon, "Influence of calcined clay/limestone, sulfate and clinker proportions on cement performance," *Construction and Building Materials*, vol. 251, p. 119050, Aug. 2020, doi: 10.1016/j.conbuildmat.2020.119050.

[26] X.-Y. Wang, "Evaluation of the properties of cement–calcined Hwangtoh clay–limestone ternary blends using a kinetic hydration model," *Construction and Building Materials*, vol. 303, p. 124596, Oct. 2021, doi: 10.1016/j.conbuildmat.2021.124596.

[27] S. Krishnan, A. C. Emmanuel, and S. Bishnoi, "Hydration and phase assemblage of ternary cements with calcined clay and limestone," *Construction and Building Materials*, vol. 222, pp. 64–72, Oct. 2019, doi: 10.1016/j.conbuildmat.2019.06.123.

[28] H. Du and S. D. Pang, "High-performance concrete incorporating calcined kaolin clay and limestone as cement substitute," *Construction and Building Materials*, vol. 264, p. 120152, Dec. 2020, doi: 10.1016/j.conbuildmat.2020.120152.

[29] N. Nair, K. Mohammed Haneefa, M. Santhanam, and R. Gettu, "A study on fresh properties of limestone calcined clay blended cementitious systems," *Construction and Building Materials*, vol. 254, p. 119326, Sep. 2020, doi: 10.1016/j.conbuildmat.2020.119326.

[30] Y. Sun *et al.*, "Development of a novel eco-efficient LC2 conceptual cement based ultra-high performance concrete (UHPC) incorporating limestone powder and calcined clay tailings: Design and performances," *Journal of Cleaner Production*, vol. 315, p. 128236, Sep. 2021, doi: 10.1016/j.jclepro.2021.128236.

[31] C. Yu, Z. Li, and J. Liu, "Degradation of limestone calcined clay cement (LC3) mortars under sulfate attack," *Low-carbon Mater. Green Constr.*, vol. 1, no. 1, p. 4, Feb. 2023, doi: 10.1007/s44242-022-00003-1.

[32] J. Yu, H.-L. Wu, D. K. Mishra, G. Li, and C. K. Leung, "Compressive strength and environmental impact of sustainable blended cement with high-dosage Limestone and Calcined Clay (LC2)," *Journal of Cleaner Production*, vol. 278, p. 123616, Jan. 2021, doi: 10.1016/j.jclepro.2020.123616.

[33] W. Zhou, S. Wu, and H. Chen, "Early Strength-Promoting Mechanism of Inorganic Salts on Limestone-Calcined Clay Cement," *Sustainability*, vol. 15, no. 6, p. 5286, Mar. 2023, doi: 10.3390/su15065286.

[34] Y. Chen *et al.*, "Rheology control of limestone calcined clay cement pastes by modifying the content of fine-grained metakaolin," *Journal of Sustainable Cement-Based Materials*, pp. 1–15, Feb. 2023, doi: 10.1080/21650373.2023.2169965.

[35] K. E. H. Eldahroty, A. A. Farghali, N. Shehata, and O. A. Mohamed, "Valorification of Egyptian volcanic tuff as eco-sustainable blended cementitious materials," *Sci*

Rep, vol. 13, no. 1, p. 3653, Mar. 2023, doi: 10.1038/s41598-023-30612-0.

[36] Y. Dhandapani, T. Sakthivel, M. Santhanam, R. Gettu, and R. G. Pillai, "Mechanical properties and durability performance of concretes with Limestone Calcined Clay Cement (LC3)," *Cement and Concrete Research*, vol. 107, pp. 136–151, May 2018, doi: 10.1016/j.cemconres.2018.02.005.

[37] M. D. Sheikh, T. Jamil, T. Ayub, A.-R. Khan, S. M. Bilal, and C. Hu, "Comparative Study on LC3-50 with OPC Concrete Using Raw Materials from Pakistan," *Advances in Materials Science and Engineering*, vol. 2023, pp. 1–10, Feb. 2023, doi: 10.1155/2023/5503670.

[38] K. A. Alfalous and M. M. Aburzeza, "Mechanical and Hydration Characteristics of Blended Cement Pasts Containing Burnt Clay".

[39] A. Hagrass, S. Ibrahim, F. El-Hosiny, S. Youssef, and M. Moharam, "Hydration Characteristics of Blended Cement Containing Metakaolin," *The Bulletin Tabbin Institute for Metallurgical Studies (TIMS)*, vol. 107, no. 1, pp. 38–51, Feb. 2018, doi: 10.21608/tims.2018.199446.

[40] S. S. Ibrahim, A. A. Hagrass, T. R. Boulos, S. I. Youssef, F. I. El-Hossiny, and M. R. Moharam, "Metakaolin as an Active Pozzolan for Cement That Improves Its Properties and Reduces Its Pollution Hazard," *JMMCE*, vol. 06, no. 01, pp. 86–104, 2018, doi: 10.4236/jmmce.2018.61008.

[41] F. Bahman-Zadeh, A. A. Ramezanianpour, and A. Zolfagharnasab, "Effect of carbonation on chloride binding capacity of limestone calcined clay cement (LC3) and binary pastes," *Journal of Building Engineering*, vol. 52, p. 104447, Jul. 2022, doi: 10.1016/j.jobe.2022.104447.

[42] P. Mokhtari, "NEW LOW COST AND GREEN COMPOSITE BINDER FOR CONSTRUCTION (Doctoral Dissertation)." 2019. [Online]. Available: https://research.sabanciuniv.edu/id/eprint/39755/1/10295048_Mokhtari_Pozhhan.pdf